RESEARCH PAPER

The Influence of Heat Treatment and High Energy Ball Milling on Density, Hardness, and Wear Behavior of Al 7150 Alloy via Hot Uniaxial Compaction

M. Abdur Rahman*, Serajul Haque

* *abdurrahman@crescent.education*

Department of Mechanical Engineering, B.S Abdur Rahman Crescent Institute of Science & Technology, India

Received: January 2022 **Revised: April 2022** **Accepted: May 2022**

DOI: 10.22068/ijmse.2618

Abstract: *The effect of the milling time and ageing on the hardness, density, and wear characteristics of Al 7150 alloy specimens made via powder metallurgy was studied. The different constituents of Al 7150 alloy were processed in a planetary ball milling set up with a BPR of 10:1 for 5, 10, and 20 hrs. At 400°C, the milled powders were subsequently hot compacted in a punch die setup. The hot-pressed specimens were solutionized initially, then aged artificially at 115°C for 3, 6, 12, 24, 30, 45, 60, and 96 hrs. The relative density was inversely proportional to the milling time. Microhardness tests showed a maximum VHN of 255 for the 24 h aged T6 specimens produced from 20 h milled powders whereas the non-aged specimens, made from unmilled 7150 alloy powders showed a VHN of 40. However the samples showed a decline in microhardness beyond 24 h of ageing. Under various conditions of sliding distance and loading conditions, the samples subjected to T6 aging showed a reduced volumetric wear rate indicating the beneficial effect of artificial aging up to 24 hrs. The volumetric wear rate gradually declined for the samples aged beyond 24 hrs of aging. The HRTEM studies revealed a high density of uniformly scattered ($MgZn_2$) precipitates in the base matrix, as well as ($MgZn_2$) phases precipitating along grain boundaries. The presence of such second phase precipitates in the matrix improved the wear characteristics of the alloy matrix. The results showed that with the optimization of process parameters such as milling time, ageing as well as reducing the particle size of the base powders, the hardness and wear behavior of Al 7150 alloy may be improved.*

Keywords: *Hardness, compaction, ball milling, Al 7150 alloy, Wear, Aging.*

1. INTRODUCTION

Owing to its remarkable strength-to-weight ratio, Al 7XXX series alloys built on the Al–Zn–Mg–Cu systems are widely employed in the aviation and automobile sectors for structural parts [1, 2]. To meet the growing need for upgraded and improved functionality of such alloys in the automotive and aerospace industries, material researchers must create a novel manufacturing route for further improving its wear and mechanical properties of these materials. The mechanical & wear behavior of these Al 7XXX series alloys can be improved further by reducing the grain structure to nanoscale regime, as established in the literature [3–6]. Heat treatment process has a significant impact on the morphologies and properties of the Al 7XXX alloy, which is an age hardenable alloy [7–9]. The Al 7150 alloy is one of the 7XXX alloys that has been extensively employed in aviation and automotive applications [10]. To produce a nanocrystalline powder with high solid solubility, a powder metallurgical technique [11] can be applied. Mechanical properties might be improved utilizing this approach caused by the formation of finer grains that are evenly distributed in the base matrix [12–14]. Ball milling causes the particles to be continuously cold-welded, broken and rewelded. As the milling process progresses, a compromise between welding and particle disintegration is attained [15]. There is no segregating or clustering of the reinforcement material as a consequence of the homogenous distribution of the strengthening media in the base alloy induced by ball milling [16, 17]. The impact between both the ball and the powdered particles lies at the heart of the ball milling process. As a result, the powder's ultimate structure is determined by the collisions, in which deformation occurs owing to repetitive fracture of milled metal powder. The mechanical performance, crystalline phase, or stress-state throughout milling significantly affect the performance of the milling process [18]. HEBM accompanied by thermal treatments promotes the formation of multiple phases, increasing the samples' hardness [19]. During the consolidation of metal powder into pellets, a variety of processes such as spark plasma sintering,

[DOI: 10.22068/ijmse.2618]

explosive compaction, hot compaction, and others are employed [20–24]. Among some of the numerous processes, high energy ball milling is a crucial large-scale manufacturing technique for creating novel materials with ideal properties. Elemental powders of micro size are subjected to high intensity ball milling to produce alloy powders of nanoscale level. Mechanical milling is used to develop nanocrystalline powders by adjusting several factors such as process control agents, ball to powder ratio, and milling time [25]. Deformation of ductile particles arises in the mechanical milling operation, while fracturing of brittle particles happens. In ball milling, the brittle particles fill the area between the ductile particles once they are cold-welded [26]. The fragmentary particles fill in the gap between the cold welded particles' inter-facial boundaries caused by the accumulation of laminar particles, the structure of the particles gets altered. When milling continues, a steady-state balance between welding and fragmentation is achieved, leading to the emergence of randomly distributed inter-facial grain boundaries. The increased refinement of particle morphology occurs in this steady-state condition [27]. Furthermore, particle size reductions accelerate the amount of diffusion within interfacial regions of nano-crystalline particles, resulting in solid solutions [31].

The milling temperature, speed, time, environment, and milling medium all play a significant part in the milled powders' eventual quality. The period of milling influences grain structure, phase change, and morphology of milled alloy powders. The use of nanotechnologies to refine the particle size of alloys has become increasingly important in the development of components with improved behavior [28]. M Abdur Rahman and N Sirajudeen explored the impact of heat treatment, particle size and volume fraction of alumina on the microhardness & wear resistance of Al 7150 alloy composite via powder metallurgy route. It was demonstrated that the T6 treated composite samples performed well in terms of increase in hardness and wear resistance [29]. Fulin Jiang et al. studied the kinetics of dynamic and static softening during multistage hot deformation of 7150 aluminum alloy [30]. Zhanying Guo et al. explored the effects of two-step homogenization on precipitation behavior of Al_3Zr dispersoids and recrystallization resistance in 7150 aluminum alloy.In compared to standard one-step homogenised specimens, the investigation found that at all annealing temperatures, a smaller recrystallized grain size and lower recrystallized fraction were achieved [31]. Xigang Fan et al. 2007 studied the influence of microstructural evolution on the corrosion and mechanical behaviour of 7150 alloy following various forms of ageing has been investigated. OM and HRTEM measurements were used to examine changes in the morphology. According to the findings, the strength and corrosion resistance of the material can be increased by optimising the ageing condition [32]. Abdur Rahman et al. studied the microhardness and wear resistance of Al 7150/SiC alloy composite via hot compaction under the effects of ageing, different compaction pressures, particle size and vol.% of SiC reinforcement.The results showed that the microhardness and wear resistance of the composites were impacted both by the addition of varying vol. % and particle size of SiC and the occurrence of precipitation hardening [33]. When Jin et al. investigated the hot deformation behaviour of 7150 aluminium alloy during compression at high temperatures, they discovered extended grains with serrations emerging in the grain boundaries. The primary basis for flow softening at low Z values include dynamic recovery and recrystallization, however the flow softening at high Z values has been attributed to dynamic precipitation and subsequent dynamic particle coarsening [34]. Although many research papers have been published on the Al 7150 alloy as shown earlier but not much research has been focused on the effect of particle size reduction of the base elemental powders of the Al 7150 alloy as well as the impact of artificial ageing on the samples produced via hot uniaxial compaction route on its microhardness and wear behavior. Thus this paper explores the influence of the milling period and artificial ageing on the morphology, phase transition, relative density, particle size, microhardness, and wear resistance of hot pressed specimens produced from Al 7150 alloy powders milled for 0, 5, 10, and 20 hours, with particle size reduction as a major factor. The above tests were conducted before and after subjecting the samples to heat treatment (artificial ageing). XRD, FESEM, and HRTEM analyses were used to characterize the samples' microstructure.

[DOI: 10.22068/ijmse.2618]

2. EXPERIMENTA PROCEDURE

2.1. Fabrication of Al 7150 alloy specimens

The chemical composition of the Al 7150 alloy is as follows: Al- 88.265%, Cr- 0.04%, Cu- 2.3%, Fe- 0.15%, Mg- 2.35%, Mn- 0.1%, Si- 0.12%, Ti- 0.06%, Zn- 6.5%, Zr- 0.115%.

Al 7150 alloy specimens were made utilizing the HEBM approach in a Retsch PM-200 planetary ball mill with jars containing WC balls. The milling duration of 5, 10, and 20 h were employed on Al 7150 alloy base elemental powder (0.5 μm) provided from Alfa Aeser, USA.

Alfa Aeser, USA, provided pure commercial aluminium powder as well as other constituent powders such as copper, chromium, iron, manganese, silicon, zinc, magnesium, titanium, and zirconium, which were combined with the required percentages as described above. The powders were milled in steel vials for 5 hours, 10 hours, and 20 hours at 300 RPM in a wet (toluene) medium, with a ball to powder ratio of 10:1. To reduce the temperature increase, a 20 minute cooling break was provided after every 20 minutes of milling. According to the literature survey [25] a higher BPR or higher speed helps in the accomplishment of quicker milling kinetics nonetheless attrition and contamination pick up from the milling media possibly will happen. Since only a small quantity is being milled in the present study, the milling speed was chosen as 300 RPM with a BPR of 10:1 [25].

A punch and die arrangement was used to accomplish hot uniaxial compaction at 400°C with a pressing load of 500 MPa and a retention period of 1 h. The die's outer diameter and height were 100 and 150 mm, respectively. A heating coil was mounted around the outside die surface, the hot compaction was carried out at 400°C.The use of boron nitride on the punch-die interface reduced friction.

2.2. Aging treatment

The chosen set of developed hot compact specimens were initially solutionized in an induction furnace at 480°C for 1 hour before being rapidly cooled in cold water. To test the effect of the artificial aging process on the samples' hardness & wear characteristics, they were subjected to an artificial age hardening/heat treatment process at 115°C for 3, 6, 12, 24, 30, 45, 60, and 96 hours.

2.3. Density measurement

The mean height of the samples was determined using a micrometer. The densities of the hot-pressed samples were determined utilizing Archimedes' principle by weighing each individually in water and air with a digital balance. The procedures were replicated 3 times to ensure that the findings were consistent.

2.4. Vickers microhardness

Upon polishing the specimens using SiC papers of various grit sizes, VHN measurements were made using a Vickers microhardness test machine (Model: MMT-X7B, Japan) at 300 gf indentation loads. After assessing the hardness in five separate points, the mean VHN measurements were obtained.

2.5. Morphology examination

The samples were polished with SiC sheets, then cleaned with water and acetone, and then etched in Keller's solution for micrographic analysis. FESEM (Brand: SUPRA40, ZEISS), & HRTEM were used to characterize the hot compacted Al 7150 alloy samples. The compacted samples were finely polished with SiC sheets with grit sizes of 800, 1200, and 1500 till their thicknesses were reduced from 60 to 70 m. Lastly, impurities were removed using acetone and methanol prior to using a Gatan Punching tool to punch out circle shaped discs (diameter: 3 mm) under gentle pressure. While using an inert gas atmosphere and milling for 30 mins, the thickness of the discs was lowered to electron transparency. HRTEM (Brand: JEOL JEM 3010 TEM, Japan) under bright field configuration with a 200 kV applied potential was used to study the morphology and crystallite size/orientation.

2.6. Wear study

The specimens' wear resistance was measured using a pin-on-disc wear tester (Model: TR20-LE, Wear and Friction Monitor, Ducom, Made in India) sliding at 1 m/s against a (62 HRC) OHNS steel disc with a 100 mm track diameter. During dry sliding wear testing sessions, the wear rate of the samples was estimated by altering the sliding distance and applied stress. The specimens had an outside diameter of 8 mm and a length of 25 mm after being machined. For varying sliding distances of 800, 1200, 1600, 2000, and 2500 m with various load conditions of 1, 2, 2.5, and 3 kg,

[DOI: 10.22068/ijmse.2618]

wear loss was calculated.

3. RESULTS AND DISCUSSION

3.1. Phase analysis

Once the milling period was extended from 5 to 20 hours, the grains became more refined. The decrease in crystallite size caused by significant permanent deformation following milling for up to 20 hours increased dislocation density [35]. $MgZn_2$ precipitate phase forms following hot pressing of 20 h processed Al 7150 alloy powder. The occurrence of phase 2 precipitates increases the hardness of the Al 7150 alloy matrix. The emergence of $MgZn_2$ precipitates due to the combined application of heat and pressure was validated by XRD examination. The specimens were removed upon cooling the specimens at ambient conditions. Earlier researches [36, 37] has described the onset of the second phase. According to XRD examination, the widening of the diffraction pattern could very well be attributable to the increase in the duration of milling from 0 to 20 hours, showing that perhaps the nano-crystalline state had been established as a result of HEBM [19]. Fig. 1 shows that in the context of a 20 hour milled specimen, the Mg_2Zn_{11} phase has precipitated. The existence of intermetallic phases may be seen in the XRD phase identification of Al 7150 alloy powders blended for specified periods of milling (0, 10, and 20 h) illustrated in Fig. 1. It's worth noting that the peaks get smaller as the milling time gets longer. Owing to 20 hours of milling, there are no peaks signaling specific components that make up the alloy matrix. The appearance of a wide halo correlating to 2 values in the band of 30° to 50°, as well as the absence of distinct peaks, indicate the nano-crystalline structure of the Al 7150 alloy powder. Yet, XRD examination of samples milled for 20 hours suggests that ball milling is likely to produce a few intermetallic phases of the nano-crystalline aggregates. Fig. 2 shows the XRD plot of hot-pressed specimens of Al 7150 alloy powders (processed for different durations), which confirms the appearance of $MgZn_2$ precipitates due to the combined application of heat and pressure throughout hot uniaxial compaction. The formation of intermetallic phases offers the hot-pressed compact enough strength. The shearing of planes of atoms causes dislocation faults to occur. Whenever the strain crosses the threshold amount in milling, it transforms it into a nanocrystalline phase [10]. The Scherrer equation and the full-width half maximum of the Aluminum peaks were used to estimate the size of the nanopowders.

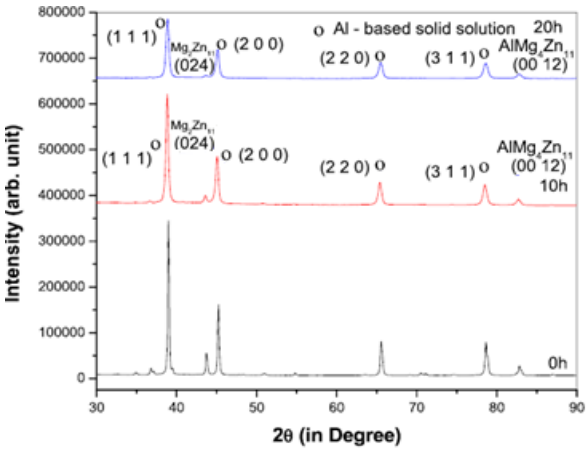

Fig. 1. XRD patterns showing the identity and sequence of phase evolution in the Al 7150 alloy powder blends during 0, 10 and 20 h of milling.

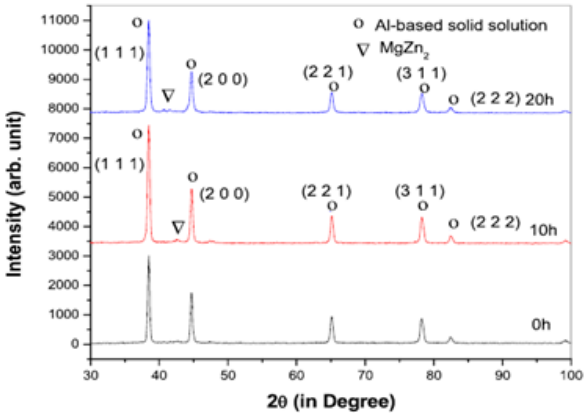

Fig. 2. XRD patterns showing the identity and sequence of phase evolution in the hot pressed compacts of Al 7150 alloy milled for a duration of 0, 10, and 20 h.

The refining of crystallite size may be validated by examining the widening of the peak when the milling time is increased, as illustrated in Fig. 3. The final particle size achieved after 20 hours of milling was 49 nm. The presence of grain refining can be established from the XRD chart and noting the widening of the peaks. Fig. 4 shows the increase in lattice strain as milling time increases. The massive plastic deformation that occurred in mechanical milling is responsible for the rise in lattice strain [38]. For each reflection, the lattice parameter (a) of the hot pressed compact alloy

[DOI: 10.22068/ijmse.2618]

was determined. The actual lattice-parameter (ap) was calculated by extrapolating the variations of the lattice-parameter as a function of the Nelson–Riley (N–R) parameter ($\cos2\theta/\sin\theta + \cos2\theta/\theta$) [39].

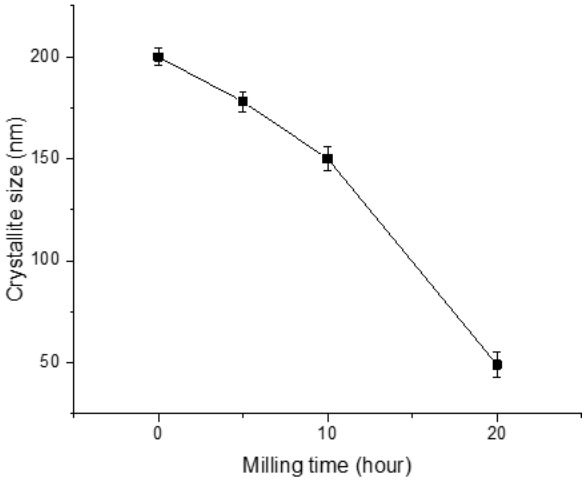

Fig. 3. Variations of crystallite size of hot compact specimens of Al 7150 alloy as a function of milling time of upto 20 h.

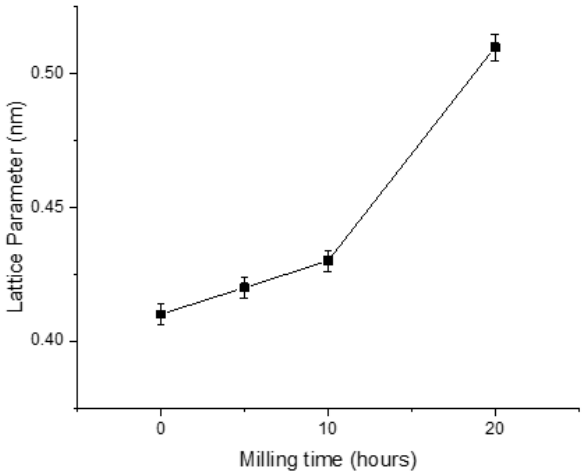

Fig. 4. Variations of lattice parameter (nm) of hot compacts of Al 7150 alloy as a function of milling time up to 20 hours.

3.2. Relative density

Fig. 5 depicts the influence of the milling period on the relative density of hot compact samples. The change in powder morphology from an irregularity towards a more spherical form is connected to the drop in relative density as milling time increases. The surface area increased as a result of this. Previous studies have reported a similar scenario for aluminum alloys based on volume porosity [40, 41].

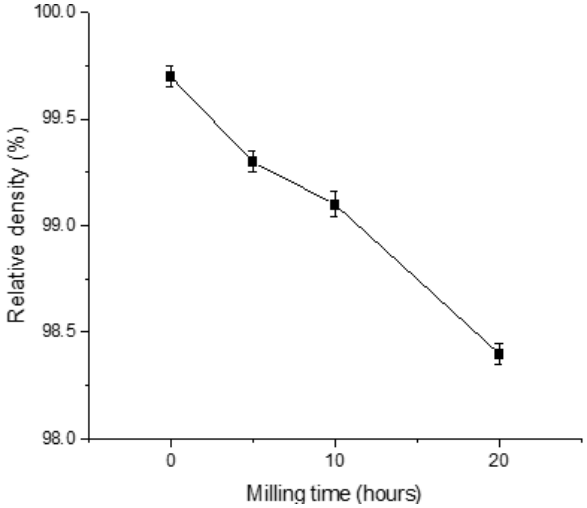

Fig. 5. Relative density of hot compact of bulk Al 7150 alloy specimens after 0, 5, 10, and 20 hours of milling.

3.3. Effect of artificial aging on the microhardness

Fig. 6 shows that increasing the milling time enhances the Vickers-microhardness of the non aged samples. This is due to the particle size reduction due to increasing the duration of milling as well as close packing of the powders under the influence of the simultaneous application of pressure and heat during hot pressing [42].

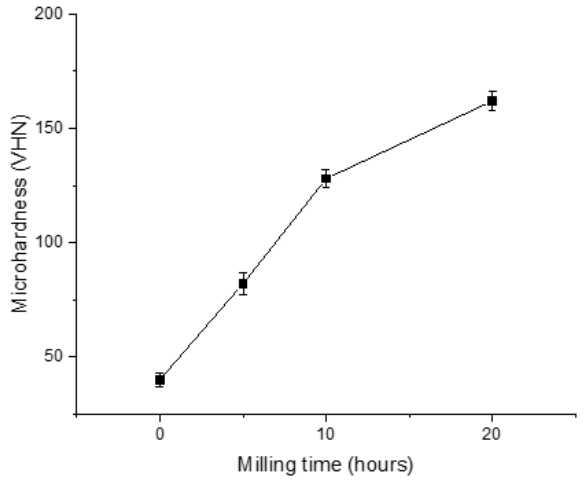

Fig. 6. Vickers microhardness of hot compact specimens of Al 7150 alloy (prior to aging) as a function of milling time up to 20 hours.

The effects of thermal treatment on the microhardness (VHN) readings of Al 7150 alloy composite samples is plotted in Fig. 7. Following solutionization, the instantly cooled specimens subsequently were artificially aged at 115°C for

[DOI: 10.22068/ijmse.2618]

specific periods of 3, 6, 12, 24, 30, 45, 60, and 96 hours. VHN analysis was carried out on the samples after various stages of heat treatment. Owing to the precipitation hardening phenomena, the microhardness of all the specimens steadily enhanced after 3, 6, 12, and 24 hours of artificial ageing.

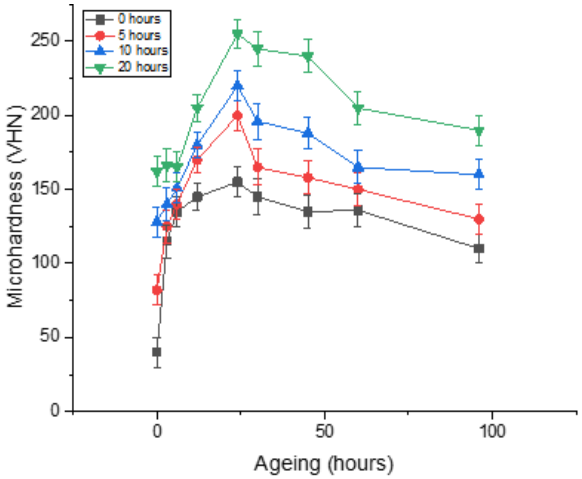

Fig. 7. Vickers microhardness of hot compact specimens of Al 7150 alloy (produced from 0, 5, 10 and 20 hour milled powders) as a function of Ageing hours.

After 24 h of artificial ageing, the peakage hardness was attained. Beyond 24 hours of ageing, the microhardness (VHN) of all specimens, regardless of particle size, began to drop (refer to Fig. 7), i.e., VHN values of 30, 45, and 60 h heat-treated specimens dropped gradually. Following 96 hours of ageing, the heat-treated specimens achieved reduced hardness values, indicating overaging. The aged specimens had superior microhardness than that of the non-aged specimens, as shown by the VHN findings (see Figs. 6-7). When compared to the other specimens, the T6 treated Al 7150 alloy made of milled powders of 49 nm had a higher microhardness of 255 VHN. The alloying elements, intermetallic compounds, (Al_2Cu), and ($MgZn_2$) are entirely soluble in the matrix during solution treatment. Clusters occur when solutionized specimens are rapidly cooled [44].

3.4. Effect of aging on wear behavior

Prior research has found that heat-treated specimens have improved wear behavior as a result of artificial ageing owing to enhanced hardness and strength [44]. Owing to the fortification of the 7150 alloy matrix, the age-hardening process results in increased wear resistance and reduced fracture nucleation characteristics [45, 46]. T6 treatment significantly increased the hardness values of AA6092/ SiC25p MMCs, boosting their wear performance, according to Gomez de Salazar and Barrena [47]. The T6 aging, which gives greater hardness and strength, prevents aluminum particles from accumulating on the steel disc surface and minimizes their deposition [48]. The draw-out of agglomerates, the lack of uniformity in the base matrix, the existence of porosity, and the poor particle-matrix contact throughout sliding activities are all variables that cause pits to develop. The aged Al 7150 alloy samples with better hardness had fewer material losses on their worn surfaces than non-aged specimens. The minimal wear loss of the aged Al 7150 alloy is attributable to matrix refinement (in nano-level), very negligible clustering problems and formation of precipitate phase during hot compaction.

As compared to the unmilled alloy, wear testing at loads of 1, 2.0, 2.5, and 3.0 kg revealed that the milled Al 7150 alloy composites had better wear resistance and hardness. Fig. 8 demonstrates the volumetric wear rate of the Al 7150 alloy and its composite specimens of non-aged specimens (as a function of different applied loads). Fig. 9 shows the volumetric wear rate of the T6 aged specimens versus different applied loads. Similarly, Fig. 10 shows the volumetric wear rate of non aged specimens as a function of various sliding distances.

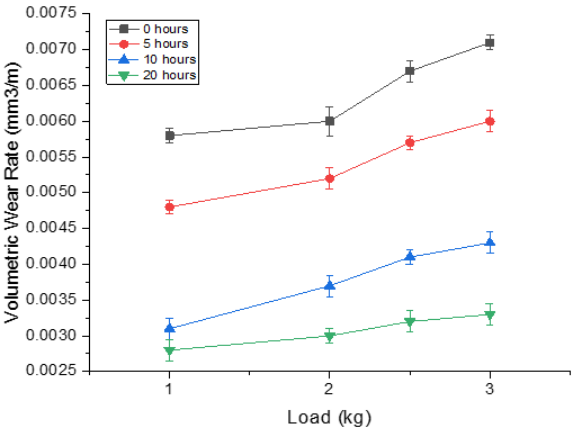

Fig. 8. Volumetric wear rate of hot compact specimens (prior to aging) produced out of Al 7150 alloy powders milled for durations of 0, 5, 10 and 20 hours at various loads during wear test.

[DOI: 10.22068/ijmse.2618]

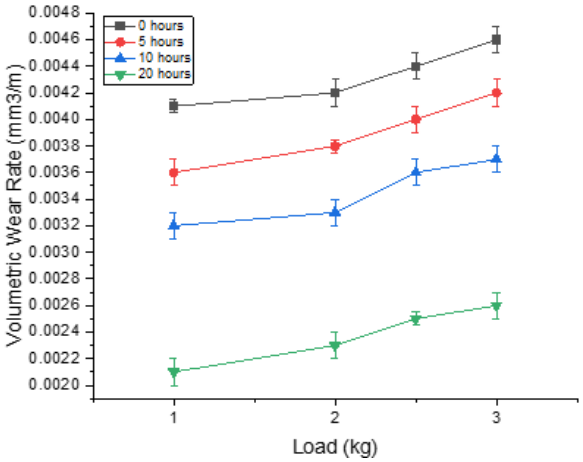

Fig. 9. Volumetric wear rate of hot compact specimens (T6 aged) produced out of Al 7150 alloy powders milled for durations of 0, 5, 10 and 20 hours at various loads during wear test.

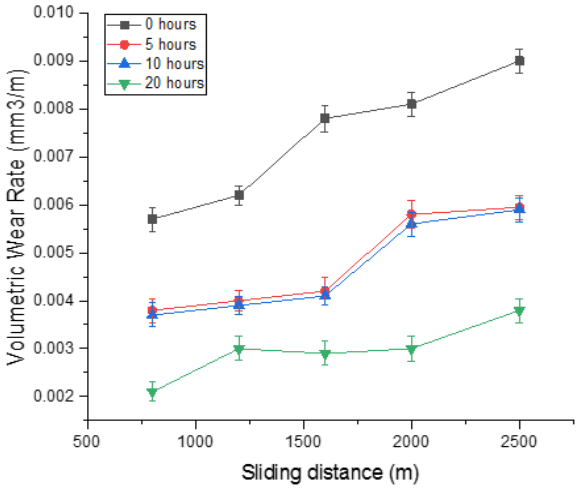

Fig. 10. Volumetric wear rate of hot compact specimens (prior to aging) produced out of Al 7150 alloy powders milled for durations of 0, 5, 10 and 20 hours (parameter: sliding distance).

Fig. 11 demonstrates the wear performance of aged samples as a function of various sliding distances The age-hardening effect causes the hardness of the specimens to improve, resulting in a lower volumetric wear rate of the T6 samples. The capacity of the prepared specimens to withstand the dry sliding wear loads throughout pin-on-disc wear testing was enhanced by the development of ($MgZn_2$) precipitates, which slowed dislocation movements [42]. The milling impact of the nanoparticles throughout sliding wear testing led to the development of iron oxides that blanketed the worn surface of the test pieces. Such iron oxide coatings which covered the specimens' surface reduced the rate of wear. The iron oxide layer's low coefficient of friction supplied in situ lubrication, preventing the contact area against severe wear [49].

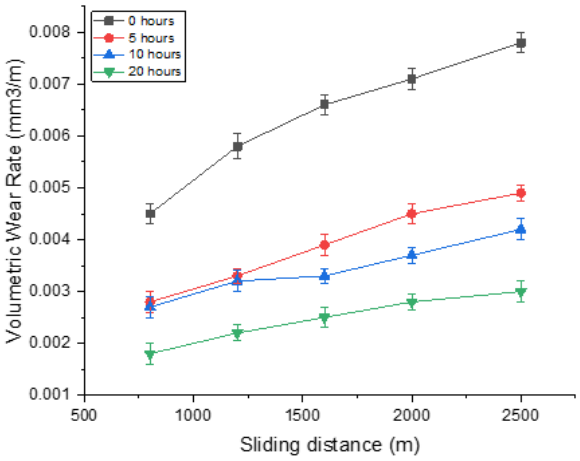

Fig. 11. Volumetric wear rate of hot compact specimens (T6 aged) produced out of Al 7150 alloy powders milled for durations of 0, 5, 10 and 20 hours (parameter: sliding distance).

3.5. Morphological analysis

HRTEM images of the 20 h processed Al 7150 alloy indicate a very dense population of η' ($MgZn_2$) precipitates dispersed uniformly in the base matrix, as well as uneven distribution of η ($MgZn_2$) precipitate phases across grain boundaries generated in hot compaction, as seen in Fig. 12. Fig. 13 illustrates the SAD configuration across the zonal axis [1 1 1], [2 0 0], [2 2 0] of Al 7150 alloy nano-crystalline 20 h milled hot-pressed sample. The small clusters grew bigger as the ageing process continued, becoming the GP zones. The GP phase gives way to the (meta-stable) η' phase. Despite the fact that smaller GP Zones exhibit increased surface energy, bigger GP Zones are much more stable than smaller ones [50]. Upon cooling the solutionized specimens, a supersaturation gets developed. Once ageing begins, the GP zones that result are evenly spread throughout the base matrix [51]. The resulting precipitate (see Fig. 2, Fig. 12-13) acts as a hindrance to dislocation motion, resulting in an increase in the hardness of the aged specimens. In most practical applications, the strengthening of the Al−Zn−Mg−Cu alloys relies on the formation of GP zones, η' phase and stable η phase precipitates [52]. Direct heterogeneous nucleation of metastable η' phase on large GP zones is not

[DOI: 10.22068/ijmse.2618]

a major mechanism for η' generation during early-stage precipitation in the alloy. Smaller GP zones have an increased surface energy, making them far more unsteady than bigger GP zones. It is well established that when the temperature rises, the precipitation formation increases. As a result, small GP zones form elongated clusters, which contribute to the emergence of η' phase, while bigger GP zones remain relatively stable and continue to grow [53]. Thus precipitates form quickly as the ageing time increases. GP zones gets dissolved in the matrix or converted to the η' phase.

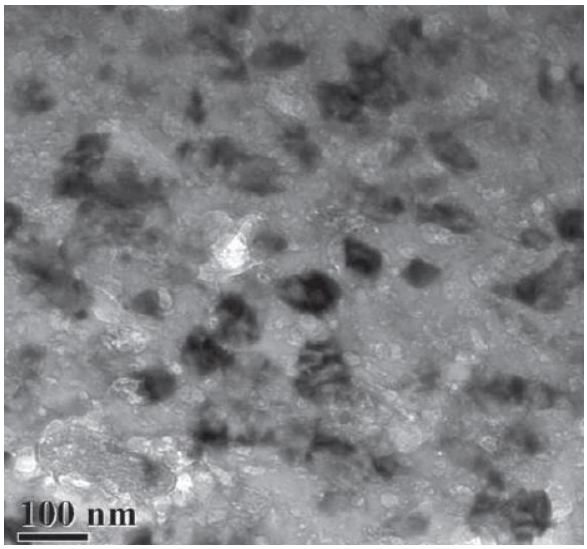

Fig. 12. Bright field TEM image of Al 7150 alloy sample (20 h milled).

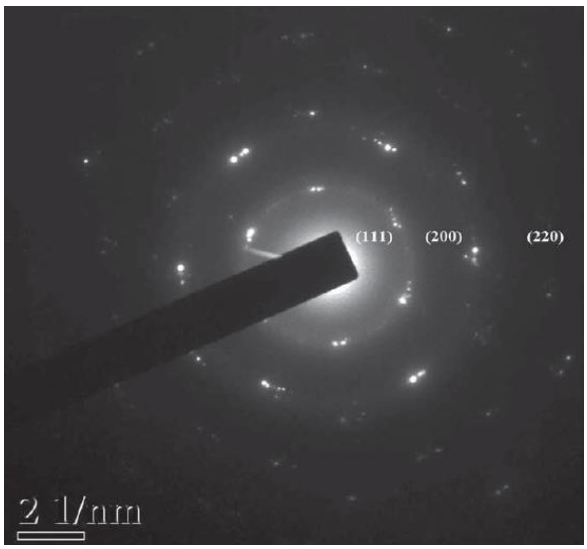

Fig. 13. Bright field TEM image of Al 7150 alloy nano-crystalline 20 h milled consolidated compact showing the SAD pattern.

The significant aspect was that after the ageing time approaches 24 hours, stable large-sized precipitates could be seen, as illustrated in Fig. 8. The following are the typical precipitation sequences [54, 55]; super saturated solid solution (SSS) → GP zones → Metastable η' phase → stable η phase. To investigate the mechanism of wear, Scanning Electron microscopy was used to assess the worn-out surfaces of the worn specimens.

FESEM images in Fig. 14– 19 clearly reveal a mixture of adhesive and abrasive wear modes. Fig. 14 shows the FESEM micrograph of non-aged Al 7150 alloy (produced from 0 hour milled 7150 alloy powder) revealing extensive damage due to plastic deformation consisting of craters, particle pull out and effects of macro ploughing indicating poor resistance to dry sliding wear.

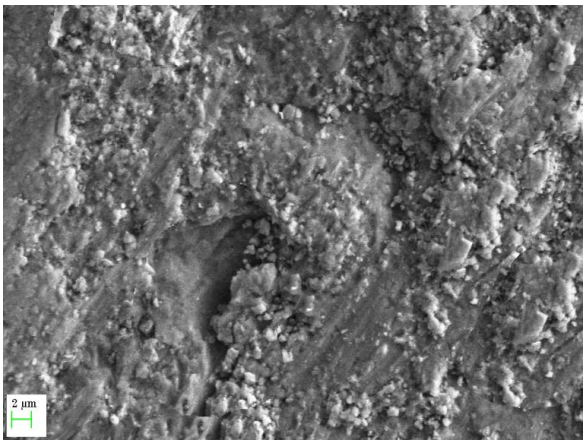

Fig. 14. FESEM micrograph of non-aged Al 7150 alloy (produced from 0 hour milled 7150 alloy powder) revealing severe damage comprising of deep grooves, craters and effects of macro ploughing.

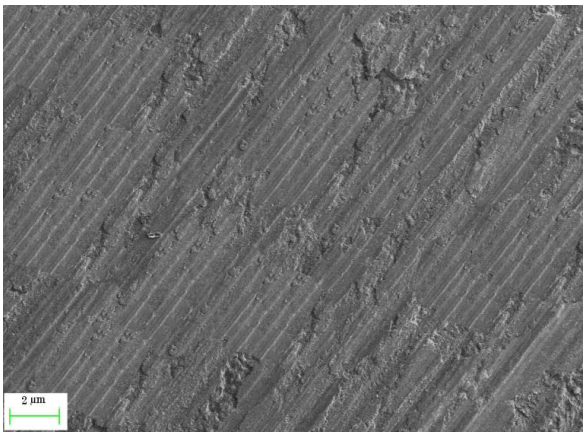

Fig. 15. FESEM image of Al 7150 alloy sample (produced from 10 h milled alloy powders) showing mild patches, grooves and effect of micro ploughing.

[DOI: 10.22068/ijmse.2618]

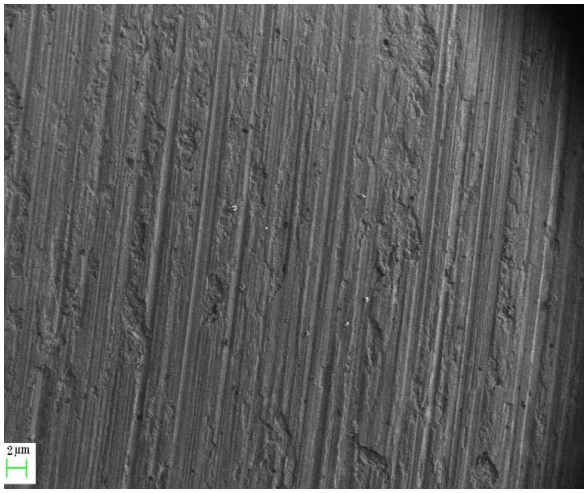

Fig. 16. FESEM image of Al 7150 alloy (produced from 20 h milled samples) showing mild patches, grooves, particle pull out, associated with mild plastic deformation.

FESEM image of Al 7150 alloy sample (produced from 10 h milled alloy powders) (refer to Fig. 15) shows mild patches, grooves that are clearly present on the surface in the sliding direction, indicating the existence of both abrasive and adhesive wear and effect of micro ploughing. When studying the wear morphological characteristics of non-heat treated samples with artificially aged specimens (refer Fig. 17-19) of Al 7150 alloy, widespread surface damage caused by extreme plastic deformation can be observed along with the growth of huge craters, denoting relatively low hardness and wear resistance of the non-aged samples. In comparison to the aged specimens, the non-aged specimen of Al 7150 alloy (refer to Fig. 14) has a heavily deteriorated surface owing to delamination type of wear, with features of macro ploughing demonstrating the development of moderate - to - severe patches.
The microstructure also indicates the non-aged Al 7150 alloy's poor wear resistance, with a substantial buildup of wear debris, craters, as well as ridges. Cavity development is caused by delamination wear, material displacement all along the sliding path, and material tearing on the sample's exterior [50]. The merging of voids led to increased levels of wear debris as the sliding progressed. This poor wear behavior can be attributed to the Al 7150 alloy's lower hardness and load-bearing capacity when compared to its milled counterpart i.e., samples made from base powders finely milled for different durations in the range of 5 to 20 hours.

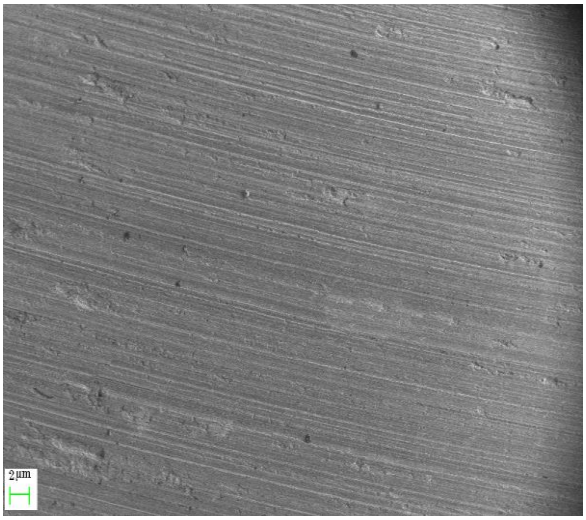

Fig. 17. FESEM image of T6 aged Al 7150 alloy (produced from 10 h milled powders) showing mild plastic deformation during sliding wear test.

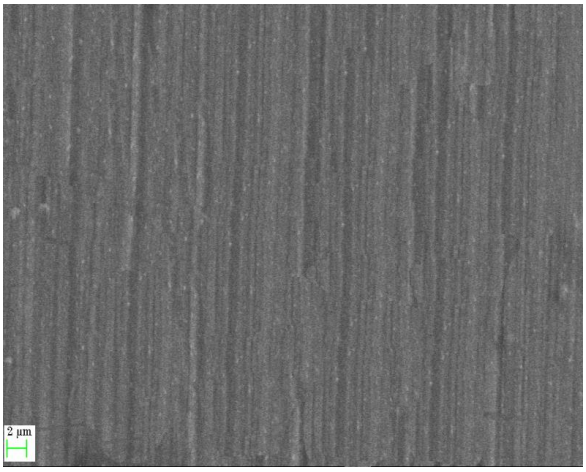

Fig. 18. FESEM image of T6 aged Al 7150 alloy (produced from 10 h milled powders) showing mild grooves indicating good wear resistance.

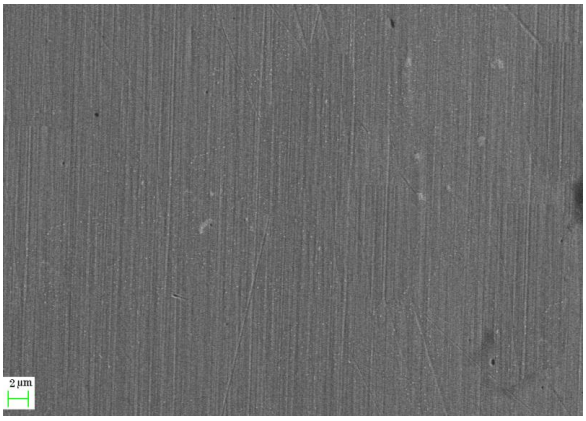

Fig. 19. FESEM image of T6 aged Al 7150 alloy (produced from 20 h milled powders) showing very negligible changes to its microstructure indicating good wear resistance.

[DOI: 10.22068/ijmse.2618]

As already stated, an increase in the milling time led to the reduction of the particle size of Al 7150 alloy powders, hence compact specimens produced from the milled powders showed micro-cracks and cavity development during the pin on disc wear tests [44].
A limited amount of delamination wear can also be seen in remote areas of the composite surface. Mechanical alloying enhances the internal energy of the particles, therefore contributing to the development of $MgZn_2$ during the hot uniaxial pressing. Another explanation for the superior performance of milled composites is the lack of agglomeration problems, which could often result in porosity [50-52]. Thus the overall effect of the milling of base powders, hot pressing, as well as artificial ageing contributed to the load-bearing capacity of the specimens during wear testing thereby showing good wear resistance of aged specimens as compared to the base Al 7150 alloy.

4. CONCLUSION

The main objective of this work was to study the effect of milling time and heat treatment on the relative density, microhardness, morphology and wear behavior of Al 7150 alloy prepared via hot compaction route. The following results were obtained:

1. According to XRD examination, the widening of the diffraction pattern could very well be attributable to the increase in the duration of milling from 0 to 20 hrs, showing that perhaps the nano-crystalline state was established as a result of HEBM. The emergence of $MgZn_2$ precipitates due to the combined application of heat and pressure was validated by XRD examination.
2. The relative density was inversely proportional to the increase in milling time which reduced the particle size from 0 to 49 nm after 20 h of milling of the base powders.
3. Owing to the precipitation hardening phenomena, the microhardness of all the specimens steadily enhanced after 3, 6, 12, and 24 hrs of artificial ageing at 115°C. Maximum hardness was attained at 24 h of ageing, beyond which the microhardness (VHN) of all the specimens, regardless of particle size, began to decline. Overageing occurred after 96 h of ageing.
4. When compared to the other specimens, the T6 treated Al 7150 alloy made of milled powders of 49 nm size showed a superior microhardness of 255 VHN. This is due to the particle size reduction due to increasing the duration of milling as well as close packing of the powders under the influence of the simultaneous application of pressure and heat during hot pressing.
5. Pin on disc wear testing conducted under varying loads and sliding speeds showed the beneficial effect of artificial ageing in enhancing the wear behavior of the T6 treated samples.
6. The capacity of the T6 specimens to withstand the dry sliding wear loads throughout pin-on-disc wear testing can be attributed to the development of ($MgZn_2$) precipitates, which slowed dislocation movements.
7. The T6 sample's HRTEM microstructure showed a high density of $MgZn_2$ precipitates dispersed evenly in the Al7150 alloy matrix, the precipitates comprising of the metastable η′ phase, with lesser amounts of GP zones and the stable ηphase were observed.
8. FESEM morphology revealed extensive damage on the wear specimen's surface due to severe plastic deformation during wear testing, indicating poor wear resistance of the non-aged samples. A mixture of adhesive, delamination and abrasive wear modes was identified during FESEM analysis.
9. The current study concludes that by optimizing the process parameters such as milling time, ageing as well as reducing the particle size of the base powders, the hardness and wear behavior of Al 7150 alloy may be improved.

REFERENCES

[1] Buha, J., R. N. Lumley, and A. G. Crosky. "Secondary ageing in an aluminium alloy 7050." Mater. Sci. Eng.: A .2008, 492, 1-10.
[2] Starke EA, Staley JT. "Application of modern aluminum alloys to aircraft." Prog Aerospace Sci 1996, 32:131–72.
[3] Valiev RZ, Islamgaliev RK, Alexandrov IV. "Bulk nanostructured materials from severe plastic deformation." Prog Mater

[DOI: 10.22068/ijmse.2618]

Sci 2000, 45, 103–109.
[4] Saito Y, Utsunomiya H, Tsuji N, Sakai T. "Novel ultra-high straining process for bulk material development of the accumulative roll-bonding (ARB) process." Acta Mater 1999, 47, 579–83.
[5] Kapoor, R., Kumar, N., Mishra, R. S., Huskamp C. S., and Sankaran, K. K., "Influence of fraction of high angle boundaries on the mechanical behavior of an ultrafine grained Al–Mg alloy." Mater Sci Eng A. 2010, 527, 5246-5254.
[6] Mishra, Rajiv S., and Z. Y. Ma. "Friction stir welding and processing." Materials science and engineering: R: reports. 2005, 50.1-2, 1-78.
[7] Srivatsan, T. S. "Microstructure, tensile properties and fracture behaviour of aluminium alloy 7150." J Mater Sci. 1992, 27.17, 4772-4781.
[8] Werenskiold, J. C., A. Deschamps, and Y. Bréchet. "Characterization and modeling of precipitation kinetics in an Al–Zn–Mg alloy." Mater. Sci. Eng.:A. 2000, 293.1-2, 267-274.
[9] Stiller, K, Angenete, J, Warren, P J, Gjoennes, J, and Hansen, V., "Investigation of precipitation in an Al–Zn–Mg alloy after two-step ageing treatment at 100 and 150 C." Mater. Sci. Eng. A. 1999, 270.1, 55-63.
[10] Pagidi Madhukar, N. Selvaraj, C.S.P. Rao, G.B. Veeresh Kumar, "Enhanced performance of AA7150-SiC nanocomposites synthesized by novel fabrication process" Ceramics International. 2020, 46.10, 17103-17111.
[11] Rahman, M. Abdur, R. Karunanithi, and N. Sirajudeen. "Sinterability and electrochemical behavior of Al_2O_3 dispersed Al 7150 alloy composite prepared by high energy ball milling." Mater. Res. Express. 2019, 6.8, 085007.
[12] Tiwari, A. N., V. Gopinathan, and P. Ramakrishnan. "Processing of modified Ai (7010)-Sic particulate composites by mechanical alloying and hot-pressing." Mater. Manuf. Process. 1991, 6.4, 621-633.
[13] Rao, C. Srinivasa, and G. S. Upadhyaya. "2014 and 6061 aluminium alloy-based powder metallurgy composites containing silicon carbide particles/fibres." Mater. Des. 1995, 16.6, 359-366.
[14] Aghili, S. E., M. H. Enayati, and F. Karimzadeh. "Synthesis of nanocrystalline (Fe, Cr) 3Al powder by mechanical alloying." Mater. Manuf. Process. 2012, 27.4, 467-471.
[15] Intrater J., Mechanical alloying and milling, c. Suryanarayana, Mater. Manuf. Process. 2007, 790-791.
[16] Cullity, B. D., & Stock, S. R. Elements of X-ray Diffraction Third Edition. Prentice-Hall. 2001.
[17] Estrada-Guel I, Carreño-Gallardo C, Mendoza-Ruiz DC, Miki-Yoshida M, Rocha-Rangel E, Martínez-Sánchez R. "Graphite nanoparticle dispersion in 7075 aluminum alloy by means of mechanical alloying." Journal of Alloys and Compounds, 2009, 483.1-2, 173-177.
[18] Cheng Chen, Congyang Lu, Xiaomei Feng & Yifu Shen, "Fabrication of Al–Si coating on Ti–6Al–4V substrate by mechanical alloying." Mater. Manuf. Process. 2018, 33.2, 186-195.
[19] Ying, D. Y., and D. L. Zhang., "Processing of Cu–Al_2O_3 metal matrix nanocomposite materials by using high energy ball milling." Mater. Sci. Eng. A. 2000, 286.1, 152-156.
[20] Rui Zhou, Li Yang, Zhong-wang Liu, Bing-fei Liu, "Modeling the powder compaction process by an integrated simulation and inverse optimization method." Mater. Today Commun., 2020, 25, 101475.
[21] Qingquan Kong, Lixian Lian, Ying Liu & Jing Zhang, "Fabrication and characterization of nanocrystalline Al–Cu alloy by spark plasma sintering." Mater. Manuf. Process., 2014, 29.10, 1232-1236.
[22] Lahiri, Indranil, and S. Bhargava. "Compaction and sintering response of mechanically alloyed Cu–Cr powder." Powder technology. 2009, 189(3), 433-438.
[23] Kumar N, Sanguino P, Faia P, Trindade B. "Porous Si-Sn alloys produced by mechanical alloying and subsequent consolidation by sintering and hot-pressing." Mater. Manuf. Process. 2022, 37.2, 169-176.
[24] Xia Li, Ding Hui, Shi Yuxiang, Ren Yaoyao, "Fabrication of dense ultrafine

[DOI: 10.22068/ijmse.2618]

TiAl alloys by spark plasma synthesis from mechanically activiated powders." Journal of Wuhan University of Technology-Mater. Sci. Ed. 2007, 22.3, 408-411.

[25] Suryanarayana, Cury. "Mechanical alloying and milling." J Progrss Mater Sci. 2001, 46.1-2, 1-184.

[26] Sharma, Pardeep, Satpal Sharma, and Dinesh Khanduja. "On the use of ball milling for the production of ceramic powders." Mater. Manuf. Process. 2015, 30.11, 1370-1376.

[27] Baskaran, S., V. and Anandakrishnan, and Muthukannan Duraiselvam. "Investigations on dry sliding wear behavior of in situ casted AA7075–TiC metal matrix composites by using Taguchi technique." Mater. Des. 2014, 60, 184-192

[28] Wang, Tao, et al. "Microstructure and mechanical properties of powder metallurgy 2024 aluminum alloy during cold rolling." J. Mater. Res. Technol. 2021, 15, 3337-3348.

[29] Rahman, M. Abdur, and N. Sirajudeen. "Influence of aging, varying particle size & volume fraction of Al_2O_3 particles on the hardness and wear behavior of Al 7150 alloy composite produced by hot uniaxial compaction method." Mater. Res. Express. 2018, 6.3: 035006.

[30] Fulin Jiang, Hui Zhang, Luoxing Li, Jianghua Chen, "The kinetics of dynamic and static softening during multistage hot deformation of 7150 aluminum alloy." Mater. Sci. Eng.: A. 2012, 552, 269-275.

[31] Ghosh, K. S., N. Gao, and M. J. Starink. "Characterisation of high pressure torsion processed 7150 Al–Zn–Mg–Cu alloy." Mater. Sci. Eng.: A. 2012, 552, 164-171.

[32] Xigang Fan, Daming Jiang, Li Zhong, Tao Wang, Shiyu Ren, "Influence of microstructure on the crack propagation and corrosion resistance of Al–Zn–Mg–Cu alloy 7150." Mater. Charact. 2007, 58.1, 24-28.

[33] Rahman, M. Abdur, N. Sirajudeen, and R. Karunanithi. "Hardness and dry sliding wear behavior of SiC reinforced Al 7150 alloy composite synthesized under the influence of aging, varying compaction pressures, particle size and volume fraction of ceramic particulates by hot compaction technique." Mater. Res. Express. 2019, 6.6, 066536.

[34] Jin, N., Hui Zhang, Yi Han, Wenxiang Wu and Jianghua Chen. "Hot deformation behavior of 7150 aluminum alloy during compression at elevated temperature." Materials Characterization. 2009, 60, 530-536.

[35] T.K. Akopyan, N.A. Belov, N.V. Letyagin, F.O. Milovich, A.A. Lukyanchuk, A.S. Fortuna, "Influence of indium trace addition on the microstructure and precipitation hardening response in Al–Si–Cu casting aluminum alloy." Mater. Sci. Eng.:A. 2022, 831, 142329.

[36] Javdani A, Pouyafar V, Ameli A, Volinsky AA. Blended powder semisolid forming of Al7075/Al_2O_3 composites: Investigation of microstructure and mechanical properties. Mater. Des. 2016, 109, 57-67.

[37] Wenbin Tu, Jianguo Tang, Lingying Ye, Lingfei Cao, Yu Zeng, Qianqian Zhu, Yong Zhang, Shengdan Liu, Lehang Ma, Jinkun Lu, Bing Yang, "Effect of the natural aging time on the age-hardening response and precipitation behavior of the Al-0.4 Mg-1.0 Si-(Sn) alloy." Mater. Des. 2021, 198, 109307.

[38] Mohamed, Farghalli A. "Correlation between the minimum grain size obtainable by ball milling and lattice strain." Mater. Sci. Eng. A. 2019, 752, 15-17.

[39] Amutha T, Rameshbabu M, Muthupandi S, Prabha K. "Theoretical comparison of lattice parameter and particle size determination of pure tin oxide nanoparticles from powder X-ray diffraction." Mater. Today: Proc. 49 (2022): 2624-2627.

[40] Salur E, Aslan A, Kuntoğlu M, Acarer M. "Effect of ball milling time on the structural characteristics and mechanical properties of nano-sized Y_2O_3 particle reinforced aluminum matrix composites produced by powder metallurgy route". Adv Powder Technol. 2021, 32(10), 3826-3844.

[41] Navas, Elisa María Ruiz, and Berta Ruiz Palenzuela." Sintering of Aluminum Alloys." Processing and Properties. 2022, 343-352.

[42] Hafenstein S, Werner E. "Pressure

[DOI: 10.22068/ijmse.2618]

dependence of age-hardenability of aluminum cast alloys and coarsening of precipitates during hot isostatic pressing." Mater. Sci. Eng.: A. 2019, 757, 62-69.
[43] Du Z, Deng Z, Xiao A, Cui X, Yu H, Feng Z. "Effect of the aging process on the micro-structure & properties of 7075 aluminum alloy using electromagnetic bulging." J. Manuf. Process. 2021, 70, 15-23.
[44] Sardar S, Karmakar SK, Das D. High stress abrasive wear characteristics of Al 7075 alloy and 7075/Al_2O_3 composite. Measurement. 2018, 127, 42-62.
[45] Deore HA, Mishra J, Rao AG, Mehtani H, Hiwarkar VD. Effect of filler material and post process ageing treatment on microstructure, mechanical properties and wear behaviour of friction stir processed AA 7075 surface composites. Surf. Coat. 2019, 374, 52-64.
[46] Singh H, Singh K, Vardhan S, Mohan S. Study on the wear performance of AA 6061 and AA 6082 based metal matrix composites. Mater. Today: Proc. 2021, 43, 660-664.
[47] De Salazar JG, Barrena MI. "Influence of heat treatments on the wear behaviour of an AA6092/SiC25p composite." Wear. 2004, 256(3-4), 286-293.
[48] Singh H, Singh K, Vardhan S, Mohan S, Singh G. "A comprehension review of dry sliding wear on aluminum matrix composites." Mater. Today: Proc. 2021. DOI:10.1016/j.matpr.2021.11.312.
[49] Praveen G, Suryakumari TS, Prasath S. "A comparative study of wear features for Al-6061/Al-2024/Al-7075 composites-A review." Mater. Today: Proc. 2020. DOI:10.1016/j.matpr.2020.10.197.
[50] Padap AK, Yadav AP, Kumar P, Kumar N. "Effect of aging heat treatment and uniaxial compression on thermal behavior of 7075 aluminum alloy." Mater. Today: Proc. 2020, 33, 5442-5447. DOI:10.1016/j.matpr.2020.03.196.
[51] Luo J, Luo H, Li S, Wang R, Ma Y. "Effect of pre-ageing treatment on second nucleating of GPII zones and precipitation kinetics in an ultrafine grained 7075 aluminum alloy." Mater. Des. 2020, 187, 108402.
[52] Chinh N Q, Lendvai J, Ping D H, Hono K. "The effect of Cu on mechanical and precipitation properties of Al−Zn−Mg alloys." J. Alloys Compd., 2004, 318(1−2): 52−60.
[53] Tanaka H. "New coarsening mechanisms for spinodal decomposition having droplet pattern in binary fluid mixture: collision-induced collisions." Phys Rev Lett, 1994, 72(11):1702−1705.
[54] Li X Z, Hansan V, Gjonnes J, Wallenberg L R. "HREM study and structure modeling of η′ phase, the hardening precipitates in commercial Al−Zn−Mg alloys." Acta Mater, 1999, 47(9): 2651−2659.
[55] Gang S, Cerezo A. "Early-stage precipitation in Al−Zn−Mg−Cu alloy (7050)." Acta Mater, 2004, 52: 4503−4516.

[DOI: 10.22068/ijmse.2618]